Soft Matter

PAPER

View Article Online
View Journal | View Issue

Cite this: *Soft Matter*, 2024, **20**, 1905

Poly(*N*,*N*-diethylacrylamide)-endowed spontaneous emulsification during the breath figure process and the formation of membranes with hierarchical pores†

Di Zhou, Ping Fu, Wan-Ting Lin, Wan-Long Li, Zhi-Kang Xu and Ling-Shu Wan *

Received 28th November 2023,
Accepted 28th January 2024

DOI: 10.1039/d3sm01603j

rsc.li/soft-matter-journal

The spontaneous emulsification for the formation of water-in-oil (W/O) or oil-in-water (O/W) emulsions needs the help of at least one kind of the third component (surfactant or cosolvent) to stabilize the oil–water interface. Herein, with the water/CS_2-soluble polymer poly(*N*,*N*-diethylacrylamide) (PDEAM) as a surfactant, the spontaneous formation of water-in-PDEAM/CS_2 emulsions is reported for the first time. The strong affinity between PDEAM and water or the increase of PDEAM concentration will accelerate the emulsification process with high dispersed phase content. It is demonstrated that the spontaneous emulsification of condensed water droplets into the PDEAM/CS_2 solution occurs during the breath figure process, resulting in porous films with two levels of pore sizes (*i.e.*, micron and submicron). The emulsification degree and the amounts of submicron-sized pores increase with PDEAM concentration and solidifying time of the solution. This work brings about incremental interest in spontaneous emulsification that may happen during the breath figure process. The combination of these two simultaneous processes provides us with an option to build hierarchically porous structures with condensed and emulsified water droplets as templates. Such porous membranes may have great potential in fields such as separation, cell culture, and biosensing.

Introduction

Spontaneous emulsification, also called self-emulsification, refers to a phenomenon in which when two immiscible liquids come into contact, emulsion droplets can be spontaneously formed with very little or even no external energy input (*e.g.*, mechanical or thermal energy).[1] It has impacts in many fields such as pharmaceutics, food, chemistry, and cosmetics.[2] A typical example is the generation of O/W or W/O emulsions during the enhanced oil recovery process by spontaneous emulsification, which is more cost-effective and efficient compared with other emulsification methods.[3] The mechanism behind this phenomenon is generally agreed to be the diffusion of water (or oil) across the interface, reaching supersaturation in another phase, and subsequent nucleation and growth into small droplets.[3] The emulsions are widely used to build porous materials. Generally, amphiphilic polymers are dissolved in the continuous oil phase and act as stabilizers of the oil–water interface. After the gradual evaporation of the oil, the organic phase is solidified, and then porous materials are formed with the self-emulsified dispersed water droplets as templates for pores.[4,5]

The breath figure method also takes advantage of water droplets as templates for preparing porous materials. The breath figure process involves the condensation of water vapor because of evaporation-induced surface cooling of the organic solution. Porous structures imprinted with the shape of the condensed water droplet arrays are generated after the complete evaporation of the solvent and water.[6–8] Clearly, both spontaneous emulsification and breath figure processes are involved with phase transitions, during which heterogeneous nucleation and growth of water droplets occur.

The hierarchy of materials in porosity and morphology is the key for improved performance and sustainability in various kinds of applications.[9] Researchers have developed a series of strategies to prepare hierarchically porous films based on the breath figure technique.[6] Strategies include but are not limited to: (1) embedding with porous patterns by top-down methods (*e.g.*, loading with metal meshes);[10,11] (2) post-modification[12] or dissolving/etching selective components of the porous

MOE Engineering Research Center of Membrane and Water Treatment Technology, and MOE Key Laboratory of Macromolecular Synthesis and Functionalization, Department of Polymer Science and Engineering, Zhejiang University, Hangzhou 310058, China. E-mail: lswan@zju.edu.cn

† Electronic supplementary information (ESI) available. See DOI: https://doi.org/10.1039/d3sm01603j

films;[13,14] (3) delicate design of the experimental conditions;[15–17] (4) selective swelling of the components and successive collapse during drying;[14,18] and (5) phase separation.[19] These methods have strict requirements for raw materials and other conditions or require necessary post-treatment. Besides, spontaneous emulsification is a method to build pores with size of only tens to hundreds of nanometers (one order of magnitude smaller than pores built by the breath figure method), which provides us with a new option.

In 2014, Bae *et al.* prepared a polystyrene-*block*-poly(*N*-isopropylacrylamide) (PS-*b*-PNIPAM) porous film by the breath figure method. The commercial amphiphilic block copolymer was doped with inorganic salts, and they proposed that the high osmotic pressure in the polymer/$CHCl_3$ phase caused the spontaneous emulsification of the condensed water droplets during the breath figure process.[20] Small pores inside the skeletons of the large pores were then generated. A few other researchers have reported similar results and also claimed that the small pores in the hierarchical structures are ascribed to the emulsification of the condensed water.[21,22] The combination of the two processes to construct hierarchical structures provides the possibility to facilely adjust the pore size, which is easy-processing and avoids additional steps for template removal. However, there is a lack of knowledge of the system in which the two processes happen simultaneously. Specifically, hierarchical pores have been prepared simply by the breath figure method in some papers, while the mechanism for the formation of such structures is still unclear, in which the possible spontaneous emulsification phenomenon is neglected.[23–26]

In this work, we carried out a detailed study on the spontaneous emulsification that occurs during the breath figure process. Poly(*N*,*N*-diethylacrylamide) (PDEAM) is soluble in water and CS_2 with different solubility, which goes through coil–globule transition with increased temperature when dissolved in water. First, a new spontaneous emulsification system of water and PDEAM/CS_2 was proposed. The influences of PDEAM concentration and temperature on the self-emulsifying properties were investigated. Then, by introducing PDEAM/CS_2 into the breath figure system, it is demonstrated that the breath figure and emulsification processes happen simultaneously, resulting in hierarchically porous films. Both enhanced convection flow inside the evaporating solution and the decreased temperature accelerate the emulsification process, during which the PDEAM concentration and solidifying time of solutions play significant roles. This work provides insights for the spontaneous emulsification in the dynamic breath figure process from both theoretical and experimental perspectives, and a new method has been proposed to prepare polymer films with hierarchical pores.

Experimental section

Materials

PDEAM ($M_n \approx 22900$ Da) was synthesized as reported in our previous work.[27] The monomer *N*,*N*-diethylacrylamide (DEAM, 98%, D-Chem) was used after distillation under reduced pressure. Poly(*N*-isopropylacrylamide) (PNIPAM, M_w = 3000–4000 Da) was purchased from Bidepharm (China). The amphiphilic block copolymer polystyrene-*block*-poly(*N*,*N*-dimethylaminoethyl methacrylate) (PS_{208}-*b*-$PDMAEMA_{12}$) was also synthesized in our lab as reported.[28] Rhodamine 6G (R6G) was purchased from Aladdin (China). Solvents including carbon disulfide (CS_2), chloroform ($CHCl_3$), toluene, and benzene were purchased from Sinopharm (China) and used as received. Water was de-ionized using the ELGA LabWater system (France) with a resistivity of 18.2 MΩ cm. PET films were kindly provided by Hangzhou Tape Factory.

Preparation of water-in-CS_2 emulsions by spontaneous emulsification

The CS_2 emulsions containing hundred-nanometer-sized water droplets were generated by directly adding water onto PDEAM/CS_2 solutions with various concentrations or injecting PDEAM/CS_2 solutions into water. The emulsions in the CS_2 phase were spontaneously and gradually generated and achieved steady states after certain time without the need for vigorous shaking or ultrasonication.

Preparation of porous films by the breath figure method

PS-*b*-PDMAEMA and PDEAM were dissolved in CS_2 or $CHCl_3$ with designed concentrations. The static breath figure method was employed to build porous films in most cases. The solutions (50 μL) were cast onto PET substrates in a sealed container with a fixed relative humidity of ~90%. The dynamic breath figure method was also employed as discussed in the text. The solutions (50 μL) were cast onto PET substrates which were placed under humid airflow with different gas flow rates. After the evaporation of the solvents and condensed water, porous films were obtained.

Preparation of porous films with aerosol water droplets as templates

PS-*b*-PDMAEMA (10 mg mL^{-1}) and PS-*b*-PDMAEMA/PDEAM (10/2 mg mL^{-1}) solutions with CS_2 as solvents were first prepared. The solutions (100 μL) were cast onto PET films under ambient conditions, which were quickly transferred below the outlet of a working ultrasonic humidifier (OCA67C6S, MUJI). After only three seconds, they were quickly transferred to an environment with a relative humidity of ~20% and dried thereafter.

Characterization

Optical photographs were taken using smart phones with constant shooting parameters. The optical microscopy (DM750P, Leica) images of CS_2 solutions or emulsions were taken in a transmission mode for bright-field images and in a reflection mode for fluorescence images (water was dyed by R6G, 0.01 mg mL^{-1}) at constant shooting parameters. The emulsions were prepared in capillary tubes with an inner diameter of 0.9 mm by injecting the CS_2 solutions (1 μL) into the tubes which were pre-filled with de-ionized water. The diameter of the emulsion droplets was measured by dynamic laser scattering

(DLS, Nano-ZS, Malvern), and the water-in-CS_2 emulsion was prepared with a PDEAM/CS_2 concentration of 2 mg mL^{-1}. The interfacial tension between organic solution and water was measured by a pendent drop method using a contact angle system (DropMeter A-200 MAIST). The same instrument was used to take optical photographs of the CS_2/water interface. UV-vis spectroscopy (UV2450, Shimadzu) was used to measure the transmittance (at 550 nm) of the emulsions. Field emission scanning electron microscopy (FESEM, SU8010, Hitachi) was used to reveal the surface and cross-sectional morphology of the prepared porous films.

Results and discussion

Static observation of PDEAM-endowed spontaneous emulsification

PDEAM is a thermo-responsive water-soluble polymer. It goes through coil–globule transition upon heating when dissolved in water. The lower critical solution temperature (LCST) of PDEAM is around 31.6 °C, depending on molecular weight, concentration, *etc.* The LCST of PDEAM is close to that of the traditional thermo-responsive polymer PNIPAM (~32 °C).[27] PNIPAM possesses a secondary amide group and thus shows strong polarity and capability to form hydrogen bonds with water. PDEAM has a tertiary amide group in its repeating unit (Fig. 1a) and exhibits better solubility in less polar solvents.[29] PDEAM shows higher solubility in CS_2 at higher temperature, and the solubility is larger than 4 mg mL^{-1} at 25 °C (Fig. S1, ESI†).

It is found that the interfacial tension between water and PDEAM/CS_2 solution (2 mg mL^{-1}) is as low as 4.1 mN m^{-1}, which is much lower than that between pure CS_2 and water (48 mN m^{-1}). This indicates the strong capability of PDEAM to adsorb and orient itself at the interface. The good affinity between PDEAM and water/CS_2 offers the possibility of spontaneous emulsification. As shown in Fig. 1b, after the addition of water onto the PDEAM/CS_2 solution and leaving it under agitation-free conditions, the bottom CS_2 solution becomes turbid gradually. It takes ~40 min for the emulsion to reach dynamic equilibrium. Optical images of upside-down pendant water droplets show a difference when the environment is switched from pure CS_2 (Fig. 1c) to PDEAM/CS_2 (Fig. 1d). Shadow fluids appear in the PDEAM/CS_2 phase around the interface (Fig. 1d). The water-saturated CS_2 works well as the solvent for PDEAM (Fig. S2, ESI†), demonstrating that the clouds in the PDEAM/CS_2 solution (Fig. 1b and d) do not originate from the precipitation of PDEAM induced by water. Therefore, the shadow fluids indicate the formation of small dispersed water droplets.[5] We dyed the water phase with fluorescent R6G before the emulsification, and the red dots shown in the fluorescence microscopy image of the generated CS_2 emulsion demonstrate the existence of tiny water droplets (Fig. 1e). The above phenomena confirmed the spontaneous formation of water-in-CS_2 emulsions. The formation and evolution of the dispersed droplets in the CS_2 phase can be observed *in situ* by optical microscopy (Fig. S3, ESI†). The diameter of the dispersed water droplets shows bimodal distribution at ~10 nm and ~300 nm, as revealed by DLS (Fig. 1f).

Control experiments were further conducted to demonstrate the specificity of the spontaneous emulsification between water and PDEAM/CS_2. For example, there are limitations in the types of oils. When CS_2 is replaced by $CHCl_3$, the interfacial tension between water and PDEAM/$CHCl_3$ (2 mg mL^{-1}) is 20.0 mN m^{-1}, and there is no clouding in the bottom $CHCl_3$ phase (Fig. S4, ESI,† sample II and Fig. S5d, ESI†). The clouding in the water phase of samples II and III should result from the

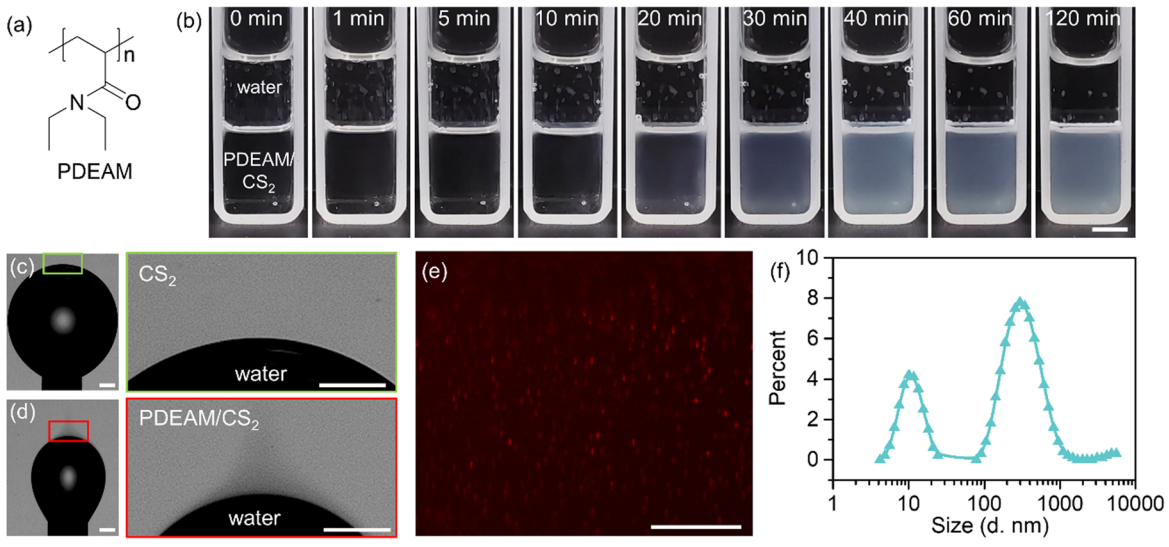

Fig. 1 (a) Molecular structure of PDEAM. (b) Typical optical photographs of the solutions (upper: pure water; bottom: PDEAM/CS_2, 1 mg mL^{-1}) at different times. (c) and (d) Optical images of upside-down pendent water droplets in (c) pure CS_2 and (d) PDEAM/CS_2 (2 mg mL^{-1}). (e) Fluorescence image of the CS_2 emulsion containing dispersed water droplets labeled by R6G. (f) DLS results of the size distributions by intensity of the dispersed droplets. Scale bars in (b) and (e) are 0.5 cm and 200 μm, respectively; scale bars in (c) and (d) are all 500 μm.

cononsolvency effect.[30] The term cononsolvency refers to the phenomenon where a polymer is less soluble in the mixture of two solvents (in this work, $CHCl_3$-containing water) than it is in either one of them (Fig. S5a, ESI†). $CHCl_3$ can disrupt the interaction between PDEAM and water, causing the collapse and aggregation of PDEAM chains.[31,32] The instant precipitation of PDEAM in the aqueous phase was also found when injecting a drop of pure $CHCl_3$ into the PDEAM/H_2O solution because of the diffusion of $CHCl_3$ into water (Fig. S5b, ESI†). Also, water will not self-emulsify into PDEAM/benzene and PDEAM/toluene solutions (Fig. S6, ESI†). Moreover, the spontaneous emulsification is direction-specific. CS_2 can diffuse and dissolve in PDEAM/H_2O solution, as the solubility of CS_2 in water is $\sim$0.1% at 20 °C, while it is not likely to form stable CS_2-in-water emulsion droplets (Fig. S7, ESI†, sample I). This phenomenon demonstrates that the initial location of PDEAM is an important parameter which will influence the spontaneous emulsification. On the other hand, whether the emulsification occurs or not is also relevant to the types of surfactants. For example, PNIPAM is soluble in both water and $CHCl_3$ (insoluble in CS_2) and can effectively decrease the interfacial tension down to 7.1 mN m^{-1} when dissolved in $CHCl_3$, while water cannot spontaneously form stable dispersed droplets in PNIPAM/$CHCl_3$ (Fig. S7, sample II, and Fig. S5e, ESI†). Similar to PDEAM, PNIPAM will also form aggregates in chloroform-containing water (Fig. S5, ESI†).

Factors influencing the spontaneous emulsification process and the mechanism

In this system we studied, it takes about 40 min for the CS_2 emulsions to reach a steady state with constantly low transmittance when no external energies are input (Fig. 1b). By recording the time-dependent transmittance of CS_2 solutions once they come into contact with water, it can be observed that the emulsifying behaviors are closely related to the concentration of PDEAM in the oil phase and the temperature of the system (Fig. 2). At a constant environmental temperature of 25 °C, optical microscopy images demonstrated that the density of emulsified micron-sized water droplets increases with the concentration of PDEAM in CS_2 when the systems reach a dynamic equilibrium (Fig. 2a). The phenomenon is also supported by the decreased transmittance of the final emulsions (Fig. 2b). An increase of concentration help to speed up the generation of obvious emulsion droplets and cause turbidity.

Interestingly, decreased temperature can also accelerate the emulsification process. At 34 °C, which is higher than the LCST of PDEAM, there is no decrease of transmittance of the CS_2 solution over 90 min (Fig. 2c). A small amount of PDEAM can gradually diffuse into the aqueous phase and then collapse to form aggregates (Fig. S8 and S9, ESI†). However, by cooling the solution to 25 °C, the CS_2 solution turns into a white haze within 6 min and the turbidity in water fades away (Fig. S9, ESI†). In this case, the emulsification rate is much greater by first heating and then cooling, since energy (heat) is introduced into the system. The switch between the clear and cloudy states of both oil and aqueous solutions with opposite direction can be constantly repeated by changing the environmental temperature.

Since there are various phase behaviors for different self-emulsification systems, the emulsification process can be instantaneous (*e.g.*, ouzo effect)[3] or slow due to kinetic barriers. Normally, the kinetic barriers can be reduced by applying external energy. In this work, the emulsification involves a few steps including diffusion of water into CS_2, supersaturation of water molecules in CS_2, and nucleation and growth of water droplets (reverse micelles) stabilized by PDEAM.[1] The opaque that forms at the interface at first are then driven into the CS_2 bulk solution by capillary flow,[33] and the aforementioned

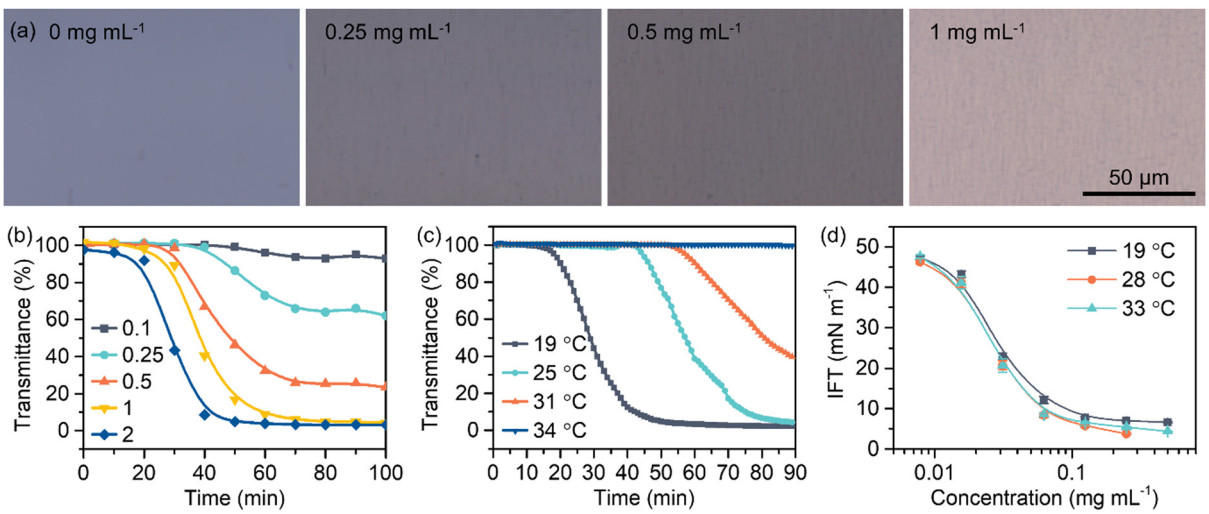

Fig. 2 (a) Bright-field optical microscopy images of resultant CS_2 emulsions with different PDEAM concentrations. (b) Time-dependent transmittance (550 nm) of CS_2 solutions with different PDEAM concentrations after being contacted with water at 23 °C. (c) Time-dependent transmittance (550 nm) of CS_2 solutions after being contacted with water at different environmental temperatures with a PDEAM concentration of 1 mg mL^{-1}. (d) Concentration-dependent interfacial tensions between PDEAM/CS_2 and water at three different environmental temperatures.

process is repeated. Therefore, the increased concentration of PDEAM in CS_2 provides the ability to stabilize a larger interfacial area, thus increasing the number of dispersed water droplets and the opacity of the emulsion. The increased PDEAM concentration also facilitates the capture and stabilization of the nuclei of water, and therefore the emulsification rate is enhanced.

Considering the dynamic feature of this process, temperature should influence the kinetic behaviors of each kind of molecule. For instance, the diffusion rate of water into CS_2 is suppressed with the decreased temperature. However, from the point of view of thermodynamics, the solubility of water in CS_2 also greatly decreases, making it easier for water that diffuses across the interface to reach supersaturation and start nucleating. Therefore, the decreased temperature is capable of promoting the emulsification process (Fig. 2c). PDEAM is rather hydrophobic at 34 °C. The hydrophile-lyophile balance (HLB) of PDEAM at 34 °C is inappropriate for the stabilization of the water-in-CS_2 interface. In this case, the water molecules that diffuse across the interface are miscible in PDEAM/CS_2, and a single phase is formed (Fig. 2c and Fig. S9, ESI†). However, once the temperature is reduced, the solubility of water in CS_2 decreases and water becomes supersaturated; thus, phase separation occurs quickly, and water starts to nucleate and generate small droplets (Fig. S9, ESI†). On the other hand, PDEAM becomes hydrophilic again and is able to act as a surfactant to stabilize water droplets. Therefore, a stable water-in-CS_2 emulsion is formed. The system becomes turbid. If the self-emulsification occurs at a constant temperature of 25 °C, it takes time for water to diffuse into the CS_2 phase and reach supersaturation, which is much slower than the process of phase separation by decreasing temperature. Once the already-formed emulsions are heated, dehydration of thermo-responsive PDEAM that locates at the water–CS_2 interface occurs.[34] The dispersed phase of water becomes unstable and water dissolves in CS_2 gradually. Hence, the cloudy emulsions disappear (Fig. S9, ESI†).

Overall, PDEAM is a non-ionic polymeric surfactant, which can significantly decrease the interfacial tension between CS_2 and water down to 4–6 mN m^{-1} when the concentration reaches 0.1 mg mL^{-1}, and it can also be adapted for other oil–water systems. It is interesting that the temperature does not show significant influence on the interfacial tension (Fig. 2d), unlike PNIPAM whose interfacial activity declines at temperature higher than its LCST[35] or ionic surfactant systems where interfacial tensions decrease with temperature.[36]

Formation of hierarchical pores by simultaneous processes of breath figure and spontaneous emulsification

The above-mentioned results demonstrate the self-emulsification of water toward PDEAM/CS_2 under experimentally static conditions. The CS_2 phase is sealed by water; and the evaporation of CS_2, so is the convection inside the liquids, is greatly suppressed. It takes ~40 min for the CS_2 emulsion to reach a steady state (Fig. 1b). Although the breath figure method is a fast-moving process, during which a solid porous film can be generated in less than 2 minutes, the various kinds of convection (*e.g.*, Marangoni flow) inside the breath figure system and the decreased temperature still provide the possibility for the condensed water droplets to self-emulsify into the CS_2 phase simultaneously.

Recently, Mathias *et al.* reported the preparation of stable W/O emulsions by directly spraying the aqueous aerosol droplets onto an oil solution.[37] With an appropriate composition of surfactants in both aqueous and oil phases and thus the appropriate interfacial tensions, the sprayed micron-sized water droplets can be successfully engulfed by oils, forming the dispersed phase and remaining stable. Herein, we also prepared water-in-CS_2 emulsions cast on PET substrates by the same method, and then the emulsions were transferred to a dry environment to allow the evaporation of CS_2 (Fig. 3a). We aimed to investigate whether the pre-engulfed water droplets will undergo self-emulsification afterwards. After the complete solidification of the solution, pores with water droplets as templates can be formed. It should be noted that, if the only solute in CS_2 solution is PDEAM, one cannot obtain porous structures since PDEAM would dissolve in water. Therefore, water-insoluble PS-*b*-PDMAEMA acts as the skeleton of the templated pores. Moreover, as an amphiphilic block copolymer, PS-*b*-PDMAEMA can decrease the interfacial tension between CS_2 and water and hence improve the stability of water droplets.[28] The time for which solutions were exposed to aerosol is rather short (3 seconds), and thus the reduction of solution temperature and time for water vapor condensation are nearly negligible,[38–40] which makes the condensed water droplets inconspicuous compared with the engulfed aerosol droplets.

The step III in Fig. 3a is similar to the normal static breath figure process in some aspects since they both involve the evaporation of the volatile solvent. We studied the morphology of the films of PS-*b*-PDMAEMA and PS-*b*-PDMAEMA/PDEAM (Fig. 3b–e). Only large pores originating from the engulfed aerosol water droplets were observed in the PS-*b*-PDMAEMA film (Fig. 3c). In contrast, when PDEAM was introduced into the CS_2 solution, it can be observed from Fig. 3e that the big pores are surrounded by a large number of small submicron-sized pores. Since the water vapor condensation should be negligible, the small water droplets (templates for the small pores) should originate from the spontaneous emulsification of the engulfed big aerosol water droplets, and this phenomenon does not exist in PS-*b*-PDMAEMA/CS_2 solution. It can be deduced that, with the aid of enhanced convection inside the cast solution and the evaporative cooling (10–20 °C lower than the environmental temperature of 25 °C),[38,39] the self-emulsification of water into CS_2 will occur within a few minutes, following the same procedure discussed in the above section.

Afterwards, we investigated the spontaneous emulsification endowed by PDEAM during the breath figure process. The emulsification degree can be distinguished by the size and density of the smaller pores from the cross-sectional SEM images of the porous films. The results are summarized in Fig. 4, 5, and Fig. S10 (ESI†), showing the influence of concentrations of both

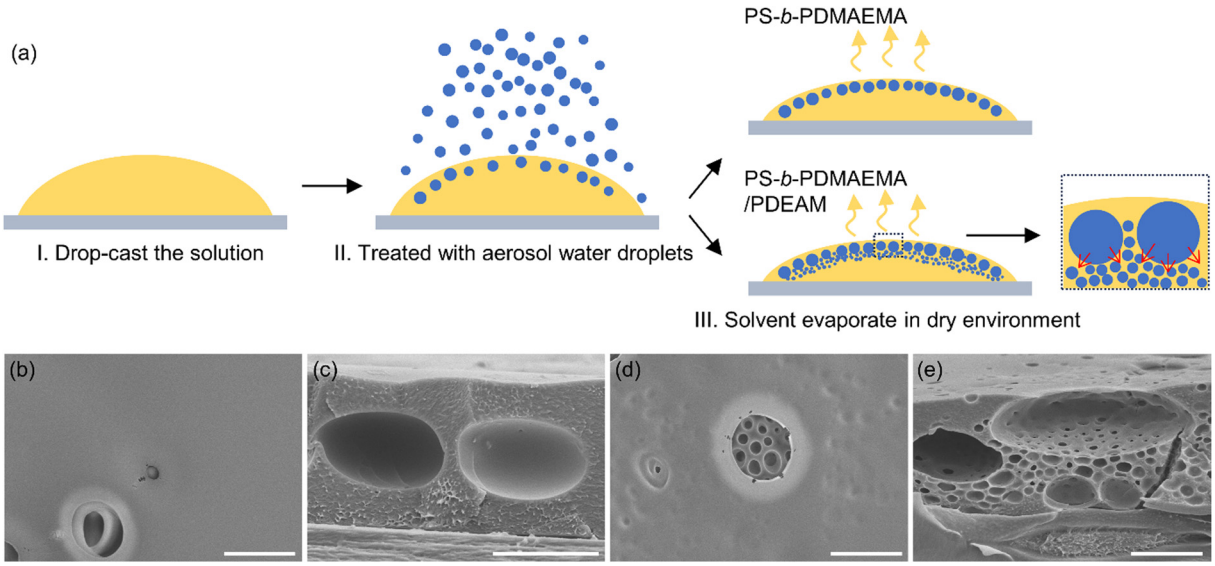

Fig. 3 (a) Schematic illustration of the process for the preparation of porous films by spraying aerosol water droplets and successive drying. (b) and (d) Surface and (c) and (e) cross-sectional SEM images of the films prepared from (b) and (c) PS-*b*-PDMAEMA (10 mg mL^{-1}) and (d) and (e) PS-*b*-PDMAEMA/PDEAM (10/2 mg mL^{-1}). Scale bars in all SEM images are 3 μm.

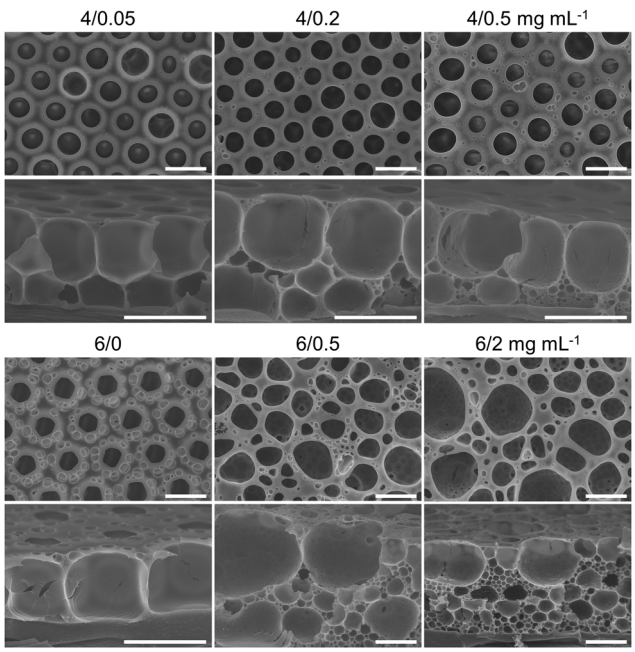

Fig. 4 Surface (upper row) and cross-sectional (bottom row) SEM images of porous films of PS-*b*-PDMAEMA/PDEAM prepared at various concentrations by the static breath figure method. Scale bars are 5 μm.

PS-*b*-PDMAEMA and PDEAM. PS-*b*-PDMAEMA shows strong capability in the stabilization of condensed water droplets during the breath figure process,[28,41] and thus leads to hexagonally packed and single-layered pores at concentrations of 2–6 mg mL^{-1} (Fig. 4 and Fig. S10, ESI†). The small surface pores around the large pores on "6/0" and "4/0" films originated from the second round of water vapor condensation (Fig. 4 and Fig. S10, ESI†). Water vapor can nucleate and grow into droplets at the places that are not occupied by previously formed water droplets before complete solidification. For the "2/0" sample, the solidifying time is shorter and there is not enough time for the second round of condensation. However, it can be observed that the regularity of surface pores is deteriorated to different extents when PDEAM is introduced (Fig. 4). It originated from the extremely low oil–water interfacial tension. In this case, the condensed water droplets will overspread and tend to coalesce with each other, which is unfavorable for producing droplets with even size.[42,43] Additionally, pores whose sizes are one order of magnitude smaller appear in the skeleton. For multi-layered porous films generated by the conventional breath figure method, the pore size is generally close or decreasing by gradient from bottom to top because of the natural nucleation-growth-submergence process experienced by each water droplet.[44–47] Both the theoretical considerations and experimental results demonstrated that small pores are the imprints of spontaneously emulsified water droplets coming from the condensed large water droplets.

By injecting water (~1.5 μL) into the CS_2 solutions, it can be observed that the shadow fluids near the interface appear earlier with the increase of PDEAM concentration (Fig. S11, ESI†). For example, when the PS-*b*-PDMAEMA/PDEAM concentrations are 4/2 mg mL^{-1}, the shadow fluid appears apparently in 15 s, which indicates the rapid formation of self-emulsified water droplets. The shadow fluids become darker with PDEAM concentration, demonstrating a larger amount of dispersed water. This phenomenon is consistent with the aforementioned static observations, *i.e.*, the increased concentration of PDEAM in the oil phase accelerates the emulsification process. Therefore, as shown in the cross-sectional SEM images, the number of submicron-sized pores templated by emulsified water droplets increases with the concentration of PDEAM when the

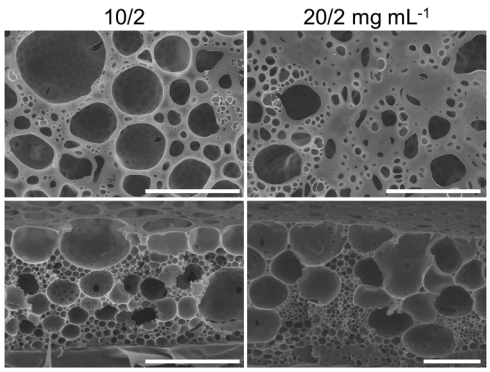

Fig. 5 Surface (upper row) and cross-sectional (bottom row) SEM images of porous films of PS-*b*-PDMAEMA/PDEAM at 10/2 or 20/2 mg mL^{-1} by the static breath figure method. Scale bars are 10 μm.

concentration of PS-*b*-PDMAEMA is fixed at 4 or 6 mg mL^{-1} (Fig. 4).

It should be noted that the decreased interfacial tension will also cause the increased nucleation rate of water vapor.[46,48] Therefore, it tends to form multi-layered condensed water droplets when PDEAM is introduced, compared with the single-layered pores of "4/0" and "6/0" films (Fig. 5 and Fig. S10, ESI†). The relatively large pores underneath the surface can also originate from the coalesced emulsified water droplets, or the uneven size distribution of the as-formed emulsified droplets. Therefore, it is worth noting that the origin of the pores with middle sizes is still vague.

In addition to PDEAM concentration, the time available for spontaneous emulsification also plays an important role. When the volume of the cast solution is fixed at 50 μL, the increase of PS concentration will slow down the evaporation of the solvent,[44] and thus prolong the solidifying time of the solution and the time for emulsification. The rationality of this idea is examined by comparing the porous structures of "4/0.5" and "6/0.5" films (Fig. 4), or finding out the significant differences between "6/2", "10/2", and "20/2" films (Fig. 4 and 5). At the same concentration of PDEAM, the number of small pores increases significantly with the concentration of PS-*b*-PDMAEMA, while the size remains close. The solidifying time also shows great importance on the porous structures fabricated from solutions with different volumes (Fig. S12, ESI†). With similar spreading area of the solutions, the increased volume leads to larger solution thickness and brings about prolonged solidifying time. The amount of the submicron-sized pores increases correspondingly. Films prepared by the dynamic breath figure method at different gas flow rates also highlight the influence of solidifying time (Fig. S13, ESI†). At a low flow rate of 0.8 L min^{-1}, the porous structure is close to the one fabricated by the static breath figure method. Once the flow rate increases, the evaporation of CS_2 was accelerated, and the small pores originating from the emulsification can hardly be distinguished. Further increase of the flow rate of humid gas to 5 L min^{-1} would facilitate water vapor condensation and strengthen the convection inside the solution, forming multi-layer-stacked condensed water droplets.

Water cannot self-emulsify into PDEAM/$CHCl_3$ solution as discussed above. Therefore, when $CHCl_3$ is used as the solvent for the breath figure process, the introduction of PDEAM into the PS-*b*-PDMAEMA solution makes no difference, and hence multi-layered pores with similar structures are generated (Fig. S14, ESI†).

Due to the dynamic nature and diverse phase behaviors of the processes studied in this work, there still remain some unanswered questions and challenges. For example, we are not sure whether the coalescence of emulsified water droplets would occur during the film-forming process or not. The precise control of the pore size, size distribution, and the ordered packing of pores at both size levels still remains challenging.

Conclusions

In summary, a spontaneous emulsification system composed of PDEAM/CS_2 and water is reported for the first time; and the influencing factors including PDEAM concentration and temperature are discussed. PDEAM-endowed emulsification behavior of water is incorporated in the breath figure process, generating hierarchical pores templated by micron-sized condensed droplets and submicron-sized emulsified droplets. The porous structures obtained by solidifying a preformed water-in-PDEAM/CS_2 emulsion in a dry environment support the idea, *i.e.*, enhanced convection and evaporative cooling would accelerate the emulsification of water. Therefore, the spontaneous emulsification of condensed water droplets occurs during the breath figure process. The increases of PDEAM concentration and solidifying time of the solution are beneficial to the increase of emulsification degree, resulting in a larger number of small pores in the films. The combination of self-emulsification and the breath figure process is conceptually simple and scalable to prepare hierarchically porous materials. It should be applicable to a wide range of other spontaneous emulsification systems.

Author contributions

Di Zhou: conceptualization, methodology, investigation, and writing – original draft. Ping Fu: validation, data curation, and writing – review and editing. Wan-Ting Lin: writing – review and editing. Wan-Long Li: writing – review and editing. Zhi-Kang Xu: supervision and writing – review and editing. Ling-Shu Wan: conceptualization, resources, supervision, and writing – review and editing.

Conflicts of interest

There are no conflicts to declare.

Acknowledgements

Financial support from the National Natural Science Foundation of China (22175151 and 22375175) is gratefully acknowledged.

References

1 C. Solans, D. Morales and M. Homs, *Curr. Opin. Colloid Interface Sci.*, 2016, **22**, 88–93.
2 A. Gupta, H. B. Eral, T. A. Hatton and P. S. Doyle, *Soft Matter*, 2016, **12**, 2826–2841.
3 Z. Li, D. Xu, Y. Yuan, H. Wu, J. Hou, W. Kang and B. Bai, *Adv. Colloid Interface Sci.*, 2020, **277**, 102119.
4 K. H. Ku, J. M. Shin, D. Klinger, S. G. Jang, R. C. Hayward, C. J. Hawker and B. J. Kim, *ACS Nano*, 2016, **10**, 5243–5251.
5 X. Chen, X. Yang, D.-P. Song, Y.-F. Men and Y. Li, *Macromolecules*, 2021, **54**, 3668–3677.
6 A. Muñoz-Bonilla, M. Fernández-García and J. Rodríguez-Hernández, *Prog. Polym. Sci.*, 2014, **39**, 510–554.
7 L.-S. Wan, L.-W. Zhu, Y. Ou and Z.-K. Xu, *Chem. Commun.*, 2014, **50**, 4024–4039.
8 A. Zhang, H. Bai and L. Li, *Chem. Rev.*, 2015, **115**, 9801–9868.
9 X.-Y. Yang, L.-H. Chen, Y. Li, J. C. Rooke, C. Sanchez and B.-L. Su, *Chem. Soc. Rev.*, 2017, **46**, 481–558.
10 J. Kamei and H. Yabu, *Soft Matter*, 2017, **13**, 7834–7839.
11 H. Hung-Chieh, C. Yi-Fan, W. Shun-Fa, S. Ming-Hui, L. Yu-Liang, C. Chia-Wei, S. Teruki and C. Jiun-Tai, *Polymer*, 2021, **221**, 123636.
12 L. Ding, A. Zhang, W. Li, H. Bai and L. Li, *J. Colloid Interface Sci.*, 2016, **461**, 179–184.
13 W. Ge and C. Lu, *Soft Matter*, 2011, **7**, 2790–2796.
14 R. Takekoh and T. P. Russell, *Adv. Funct. Mater.*, 2014, **24**, 1483–1489.
15 P. S. Shah, M. B. Sigman Jr., C. A. Stowell, K. T. Lim, K. P. Johnston and B. A. Korgel, *Adv. Mater.*, 2003, **15**, 971–974.
16 H. Sun, Q. Yang and J. Hao, *Adv. Colloid Interface Sci.*, 2016, **235**, 14–22.
17 F. Gao, W. Wang, X. Li, L. Li, J. Lin and S. Lin, *J. Colloid Interface Sci.*, 2016, **468**, 70–77.
18 T. Qu, Q. Chang, D. You, M. Huang, X. Gong, J. Wang, B. Li, G. Zheng, F. Hu, F. Zhong, C. Gong and H. Liu, *Macromol. Rapid Commun.*, 2022, **43**, 2200403.
19 P. Marcasuzaa, M. Save, P. Gérard and L. Billon, *J. Colloid Interface Sci.*, 2021, **581**, 96–101.
20 J. Bae, T. P. Russell and R. C. Hayward, *Angew. Chem., Int. Ed.*, 2014, **53**, 8240–8245.
21 B. Wu, W. Zhang, N. Gao, M. Zhou, Y. Liang, Y. Wang, F. Li and G. Li, *Sci. Rep.*, 2017, **7**, 13973.
22 E. Bormashenko, Y. Bormashenko and M. Frenkel, *Materials*, 2019, **12**, 3051.
23 P. Marcasuzaa, S. Pearson, K. Bosson, L. Pessoni, J.-C. Dupin and L. Billon, *Chem. Commun.*, 2018, **54**, 13068–13071.
24 H. Ma, Y. Tian and X. Wang, *Polymer*, 2011, **52**, 489–496.
25 K. H. Wong, T. P. Davis, C. Barner-Kowollik and M. H. Stenzel, *Polymer*, 2007, **48**, 4950–4965.
26 M. Chen, G. Zhang, Z. Gao, J. Hao, S. Zhou and H. Li, *J. Phys. Chem. C*, 2018, **122**, 24851–24862.
27 D. Zhou, L.-S. Wan, Z.-K. Xu and K. Mochizuki, *J. Phys. Chem. B*, 2021, **125**, 12104–12109.
28 B.-H. Wu, L.-W. Zhu, Y. Ou, W. Tang, L.-S. Wan and Z.-K. Xu, *J. Phys. Chem. C*, 2015, **119**, 1971–1979.
29 F. L. Bian, M. Z. Liu and F. L. Sheng, *Acta Phys.-Chim. Sin.*, 2004, **20**, 337–343.
30 S. Nian and L. Pu, *Chem. – Eur. J.*, 2017, **23**, 18066–18073.
31 B. Liu, J. Wang, G. Ru, C. Liu and J. Feng, *Macromolecules*, 2015, **48**, 1126–1133.
32 K. Mochizuki, S. R. Pattenaude and D. Ben-Amotz, *J. Am. Chem. Soc.*, 2016, **138**, 9045–9048.
33 M. Schmitt, R. Toor, R. Denoyel and M. Antoni, *Langmuir*, 2017, **33**, 14011–14019.
34 F. Marchal, A. Roudot, N. Pantoustier, P. Perrin, J. Daillant and P. Guenoun, *J. Phys. Chem. B*, 2007, **111**, 13151–13155.
35 X. Li, H. ShamsiJazeyi, S. L. Pesek, A. Agrawal, B. Hammouda and R. Verduzco, *Soft Matter*, 2014, **10**, 2008–2015.
36 Z. Ye, F. Zhang, L. Han, P. Luo, J. Yang and H. Chen, *Colloids Surf., A*, 2008, **322**, 138–141.
37 M. Steinacher and E. Amstad, *ACS Appl. Mater. Interfaces*, 2022, **14**, 13952–13961.
38 H. Battenbo, R. J. Cobley and S. P. Wilks, *Soft Matter*, 2011, **7**, 10864–10873.
39 L. A. Dombrovsky, M. Frenkel, I. Legchenkova and E. Bormashenko, *Int. J. Heat Mass Transfer*, 2020, **158**, 120053.
40 F. J. Dent, D. Harbottle, N. J. Warren and S. Khodaparast, *ACS Appl. Mater. Interfaces*, 2022, **14**, 27435–27443.
41 B.-B. Ke, L.-S. Wan, Y. Li, M.-Y. Xu and Z.-K. Xu, *Phys. Chem. Chem. Phys.*, 2011, **13**, 4881–4887.
42 H. Dobbs and D. Bonn, *Langmuir*, 2001, **17**, 4674–4676.
43 Y. Fukuhira, H. Yabu, K. Ijiro and M. Shimomura, *Soft Matter*, 2009, **5**, 2037–2041.
44 L.-W. Zhu, L.-S. Wan, J. Jin and Z.-K. Xu, *J. Phys. Chem. C*, 2013, **117**, 6185–6194.
45 M. Huh, M. Gauthier and S. I. Yun, *Polymer*, 2016, **107**, 273–281.
46 D. Zhou, B.-H. Wu, W.-W. Yang, X. Li, L.-W. Zhu, Z.-K. Xu and L.-S. Wan, *J. Polym. Sci.*, 2022, **60**, 2371–2382.
47 Y. Li, Y. Cao, S. Wu, Y. Ju, X. Zhang, C. Lu and W. Sun, *Polymer*, 2023, **269**, 125731.
48 A. E. Saunders, J. L. Dickson, P. S. Shah, M. Y. Lee, K. T. Lim, K. P. Johnston and B. A. Korgel, *Phys. Rev. E: Stat., Nonlinear, Soft Matter Phys.*, 2006, **73**, 031608.